

# Magnetically applicable layered iron-titanate intercalated with biomolecules

Kai Kamada,<sup>\*a</sup> Suguru Tsukahara<sup>a</sup> and Nobuaki Soh<sup>\*b</sup>

Received (in XXX, XXX) Xth XXXXXXXXX 200X, Accepted Xth XXXXXXXXX 200X

5 First published on the web Xth XXXXXXXXX 200X

DOI: 10.1039/b000000x

We have prepared bio-inorganic nanohybrids consisting of magnetic inorganic nanolayers (iron-titanate) and protein molecules via exfoliation–restacking process in solution. It was found that the protein molecules were electrostatically and spontaneously incorporated into the interlayer space  
10 of the inorganic layered structure by adjusting the pH of the solution appropriately. The binding studies demonstrated the high affinity of the iron–titanate nanolayers for the proteins, and the immobilized protein preserved its activity after the hybridization. The catalytic activity measurement and magnetic separation experiment indicate the formation of magnetically applicable inorganic layer–biomolecule nanohybrids. The magnetic layer–biomolecule nanohybrid  
15 developed here would be a novel conspicuous material which shows different properties from those of conventional biomolecule-immobilized magnetic particles.

## Introduction

No one doubts a great contribution of magnetism to the state of the art in nanotechnology. Especially, magnetic particles  
20 are making a great success in nanobiotechnology as a new tool for magnetic resonance imaging (MRI) contrast agent,<sup>1</sup> targeted drug delivery system,<sup>2</sup> bioseparation,<sup>3</sup> and thermal tumor therapy.<sup>4</sup> In some applications, biomolecules are immobilized on the magnetic particles. Although the  
25 immobilization of the biomolecules on the magnetic particles coated with polymer or chemically stable oxide layer would improve the stability of biomolecules to some extent, the protection effect is not sufficient because the most parts of the biomolecules are exposed to outside environment. This will be  
30 a serious problem when one uses such biomolecule-immobilized magnetic particles for a long time or applies them under extreme conditions (at high temperatures, at non-physiological pHs, or in organic solvents). Inorganic materials having regular nanospaces are attractive because they have  
35 unique ability to enhance the stability of biomolecules by encapsulating them into the nanospaces. For example, it has been reported that stabilities of proteins are much improved compared to those of free proteins by using inorganic frameworks such as mesoporous materials, clay minerals, and  
40 layered metal (hydro)oxides.<sup>5–7</sup> Among them, inorganic layered materials are adaptable to hybridization of many kinds of guest molecules with various sizes via facile solution processing.<sup>8,9</sup> As the representative studies, Kumar and co-workers found that the interstratification with  $\alpha$ -zirconium  
45 phosphate layers improves chemical and thermal stabilities of proteins.<sup>10–12</sup> Generally, inorganic materials have a great potential to acquire a novel function depending on their elementary compositions. Therefore, if a new hybrid composed of biomolecules and inorganic layered materials  
50 having magnetic properties is created, this will be the innovative tool that is different from conventional magnetic

particles. Concretely, the proposed nanohybrid will accomplish stabilization and magnetization simultaneously, *i.e.*, the produced nanohybrids can effectively draw out both  
55 functions of inorganic material and biomolecule. In this study, we first explored the preparation, characterization, and functions of the inorganic magnetic layer–biomolecule nanohybrid. Enzyme was selected as a target biomolecule from the view point that the enhancement of stability for  
60 various kinds of enzyme is highly desired for applications in bioengineering and more extensive fields including biomedical fields.

## Experimental

### Synthesis and delamination of layered iron–titanate

65 Pristine  $K_{0.8}Fe_{0.8}Ti_{1.2}O_4$  (KFTO) and its derivatives were prepared according to the protocol reported by Sasaki et al.<sup>13</sup> with some minor modifications. The KFTO powder was produced by calcination of appropriate amounts of  $K_2CO_3$ ,  $Fe_2O_3$ , and  $TiO_2$  at 1100 °C for 12 h twice with intermediate  
70 grinding. The potassium ions in the KFTO (1 g) were substituted with  $H^+$  during stirring in 1 M HCl (50 ml) over 24 h. The protonated powder (HFTO) was filtered and washed with copious water. The resultant HFTO (0.1 g) was exfoliated to single FTO nanolayer by vigorous stirring in  
75 tetrabutylammonium hydroxide solution (TBAOH, 25 ml) more than 1 week, where the amount of TBAOH was equivalent to 2-fold molar excess to the ion exchange capacity of the HFTO.

### Hybridization of HRP with FTO nanolayers

80 FTO layers intercalated with enzyme, horseradish peroxidase (HRP), was formed by mixing of HRP (Wako Pure Chemical, MW: 40200) solution with the exfoliated FTO suspension. The stock solution of FTO (pH = 6, 1 mg/ml) was prepared by dilution and addition of acetic acid to the basic FTO  
85 suspension as mentioned above. The lyophilized HRP powder

was dissolved into 0.02 M acetate buffer solution with pH = 4 or 5 (0.5 – 3.0 mg/ml). Zeta potentials of the stock solutions of HRP (5 mg/l) and FTO (2 mg/l) were estimated using an electrophoretic laser light scattering spectrophotometer. The equivalent volumes of each stock solution were blended and stirred for 3 h at 308 K, where the reaction mixtures at HRP/FTO (w/w) = 1.5 showed pH = 4.3 or 5.2 according to the pHs of buffer solution. After that, the precipitate was collected by centrifugation. The dried product was obtained by washing and sequent lyophilizing. In the present study, molar concentration of FTO is expressed on the basis of the number of unit negative charge in the FTO.

### Characterizations of HRP-FTO nano hybrids

Powder X-ray diffraction (XRD) pattern of the HRP-FTO nano hybrid was recorded with Ni-filtered Cu-K $\alpha$  radiation with wavelength of 0.15418 nm (40 kV, 30 mA). The measurements were carried out for thin film samples after air-drying of the HRP-FTO suspensions on the glass plate. The morphologies of the lyophilized powders were observed using scanning electron microscopy (SEM) equipment with accelerating voltage of 5 kV. Fourier-transformed infrared (FTIR) spectra of HFTO, HRP-FTO, and free HRP powders were measured using a conventional KBr matrix technique. Magnetism of the powder sample was measured at room temperature on a vibrating sample magnetometer (VSM).

### Catalytic activity evaluations

The enzyme catalytic activity of HRP was studied using oxidation of *o*-methoxyphenol (guaiacol) as a substrate. The reaction solution was prepared by mixing of 15  $\mu$ M HRP or HRP-FTO (240  $\mu$ l) and 5 – 10 mM guaiacol (240  $\mu$ l) with 1896  $\mu$ l of 0.02 M acetate buffer solution (pH = 4) in a quartz glass cuvette (light path length: 1 cm), where The HRP-FTO nano hybrid, which was prepared at HRP/FTO = 1.5 (w/w) and pH = 4, was also employed. The formation rate of oxidation products was monitored by absorption change at 470 nm and 298 K immediately after the addition of 24  $\mu$ l of 100 mM H<sub>2</sub>O<sub>2</sub> to the solution. The relationship between substrate concentration (0.5 – 10 mM) and initial reaction rate was utilized to calculate the kinetic parameters ( $K_m$  and  $V_{max}$ ) by means of a curve fitting method.

## Results and discussion

Various kinds of positively-charged chemical species can substitute for K<sup>+</sup> ions in interlayer of the layered potassium iron-titanate (KFTO) which was used as a precursor of magnetic nanolayer. It was confirmed that a commercial permanent magnet attracts the fine powders of KFTO and its proton exchanged form (HFTO), implying the effectiveness as a magnetic host accepting biomolecules. Horseradish peroxidase (HRP) was adopted as a target biomolecule (enzyme) in the present study. The HFTO was delaminated to individual FTO nanolayers (Fe<sub>0.4</sub>Ti<sub>0.6</sub>O<sub>2</sub><sup>0.4+</sup>) via insertion of bulky tetrabutylammonium ions (TBA<sup>+</sup>), and then the exfoliated FTO nanolayers were hybridized with the HRP. More specifically, electrostatic interaction between negatively charged FTO with HRP having opposite surface charge causes

spontaneous formation of FTO lamellar structure interleaved with HRP. As well-known, charging state of solid surface strongly depends on acidity of solution. The fact indicates that the solution pH would greatly influence the formation of the

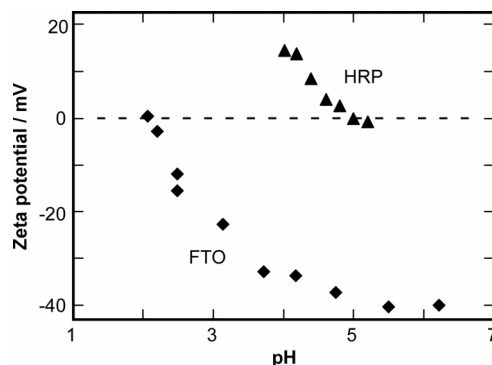


**Fig. 1** Effect of pH on zeta potentials of FTO (2 mg/L) and HRP (5 mg/L). The pH was adjusted by addition of 0.1 M HCl and 0.1 M NaOH to FTO<sub>aq</sub> (pH = 6.2) and HRP<sub>aq</sub> (pH = 4.0) as starting solutions, respectively.

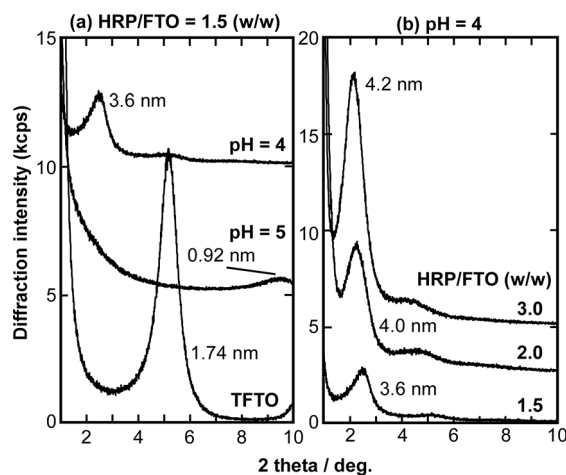


**Fig. 2** Effect of (a) synthesis pH and (b) HRP/FTO weight ratio on X-ray diffraction pattern of HRP-FTO nano hybrid. *d*-spacings are written around each peak.

HRP-FTO nano hybrids. We thus investigated the effect of solution pH on the binding of HRP to the FTO nanolayers as a first step. Zeta potential measurement is a proper technique to assess polarity and its strength of solid surface in solution. As shown in Fig. 1, the surface of exfoliated FTO nanolayer charges negatively over a wide range of pH and isoelectric point of FTO ( $pI_{FTO}$ ) is located at pH = 2, which is closed to that of layered titanate without iron.<sup>14,15</sup> In contrast, the HRP used in this study shows  $pI_{HRP} \sim 5$  that is significantly lower than those previously reported ( $pI_{HRP} = 7 \sim 9$ ).<sup>16,17</sup> Judging from these facts, the pH during the hybridization should be maintained less than 5 in order to charge the HRP surface positively.

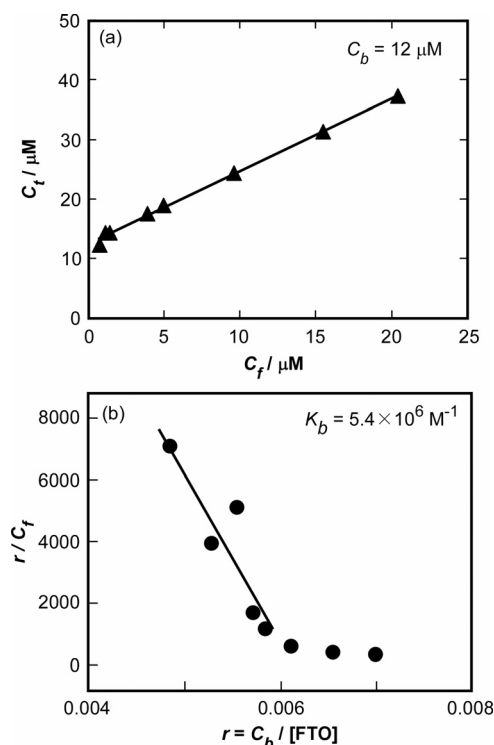
Fig. 2 depicts the X-ray diffraction (XRD) patterns of the HRP-FTO nano hybrids. The sample fabrication was carried out by simple mixing of the exfoliated FTO suspension (1.0 mg/ml) and HRP (1.5 ~ 3.0 mg/ml) dissolved in acetate buffer solution of pH = 4 or 5. The pattern of TBA<sup>+</sup>-intercalated FTO (TFTO) is also displayed for comparison. As shown in

Fig. 2a, the obtained XRD patterns were drastically altered depending on the pH. As can be seen from the figure, no discernible diffraction line was observed in the products prepared at pH = 5 independent of the HRP/FTO ratio (0.5 ~ 2.0 (w/w)), while the negligible peak attributed to (020) plane of the HFTO appeared around  $2\theta = 9.5^\circ$ .<sup>13,18</sup> The result clearly reveals a difficulty of electrostatic assembly between FTO and HRP at pH = 5 since the zeta potential of HRP is nearly zero as stated already. In contrast, when the HRP stock solution was relatively acidic (pH = 4), the broad peak of FTO structure was recognized at lower diffraction angle than that of TFTO. During the reaction, a periodical HRP/FTO layered structure was spontaneously assembled by the intercalation of positively charged HRP having a large molecular size. The peak broadening may be related to random orientation of the HRP molecules in the interlayer space. At pH = 4, the expanded layered structure was produced even at the smaller HRP/FTO weight ratio = 0.5 ( $d = 3.4$  nm). On the other hand, it was confirmed that the HRP molecules existing in the interlayer of FTO were able to be extracted by stirring in phosphate buffer solution of pH = 7.4 due to electrostatic repulsion between negatively charged HRP and FTO. The solution pH also affected the morphologies of the dried products. According to SEM observations (Fig. 1 in Supplementary Data), the round and aggregated particles were observed in the product at pH = 5, while almost particles obtained at pH = 4 retained lamellar structure. The hybridization efficiencies of HRP, *i.e.*, percentage of bound HRP amount against total, were evaluated from a comparison of absorbances at the Soret band of HRP (402 nm) for the stock solution and supernatant after centrifuging the mixture after 3 h reaction (HRP/FTO = 2.0 (w/w)).<sup>10</sup> As a result, the estimated efficiencies were 77 and 33 % at pH = 4 and 5 (308 K), respectively. The higher efficiency at pH = 4 is agreed with the results of the zeta potential and the XRD measurements. On the other hand, it was found that the synthesis temperature has only a little influence on the hybridization efficiency as compared with the solution pH (ex. 79 and 74 % at 303 and 313 K, respectively).

Fig. 2b displays the XRD patterns of HRP-FTO nanohybrids fabricated in the mixed solution with various HRP/FTO weight ratios at pH = 4. The full width at half maximum (FWHM) of the peak was narrowed at the large HRP/FTO ratio. The sharpened peak means the enhanced crystallinity of the HRP-FTO nanohybrids owing to ordered arrangement of HRP molecules in the interlayer.  $d$ -spacings were also increased with increasing the HRP/FTO ratio. The interlayer separation calculated by subtraction of FTO thickness from the  $d$ -spacing exceed a minimum dimension of HRP molecule ( $3.0 \times 3.5 \times 6.0$  nm<sup>17,19</sup>) at HRP/FTO  $\geq 2$ . In these cases, the whole HRP molecules were inserted in the interlayer spaces between the FTO nanolayers except for the surface adsorbates. As a result, it can be concluded that the simple mixing method of exfoliated FTO nanolayers and HRP at pH = 4 realizes an intercalation of HRP molecules into the FTO layered structure. The exfoliation and restacking technique of inorganic layers has been extensively studied to intercalate various kinds of guest ions or molecules. Our novel

findings with respect to the pH-dependent hybridization efficiencies would give us fundamental guidelines for immobilization of guest species (especially biomolecules) in inorganic matrix. Based on the results obtained here, the further investigations are focused on the HRP-FTO nanohybrids formed at pH = 4.

There are several papers studying on intercalation of biomolecules into layered titanate not including magnetic elements.<sup>14,15,19</sup> However, no report has dealt with chemical stoichiometry and binding constant of targeted molecules for titanate within our knowledge. In order to study affinity of HRP for magnetic FTO nanolayer, binding parameters were determined by means of the simple centrifugation method described else.<sup>20</sup> Briefly, the reaction mixtures with various HRP/FTO weight ratios were centrifuged after stirring for 3 h to settle the nanohybrids. The HRP/FTO ratio in the



**Fig. 3** Affinity of HRP for FTO layer. (a) Plot of total HRP concentration ( $C_t$ ) against free HRP ( $C_f$ ) after 3 h reaction. The vertical intercept of the linear fitting corresponds to stoichiometry of HRP ( $C_b$ ) for FTO (2.4 mM). (b) Scatchard analysis of HRP binding to FTO. Binding constant ( $K_b$ ) can be calculated from slope of linear regression at low  $r$  region ( $-K_b$ ).

precipitate was indirectly estimated by measuring free HRP concentration remaining in the supernatant as identical manner stated above. Fig. 3a shows the plot for determination of binding stoichiometry. The free HRP concentrations ( $C_f$ ) were constantly lower than the total concentration ( $C_t$ ), supporting the presence of HRP in the product. The linear relationship in Fig. 3a means facile control of the binding amount. The binding stoichiometry ( $C_b$  corresponds to  $C_t$  at  $C_f = 0$ ) estimated from vertical intercept was about  $12 \mu\text{M}$  for 2.4 mM FTO. The obtained  $C_b$  largely exceeds that of mesoporous silica,<sup>6</sup> and thus the high capacity may be advantage of the

FTO and other exfoliated nanolayers. The equilibrium binding constant ( $K_b$ ) of HRP was also determined by the Scatchard equation (eq. (1)).<sup>21</sup>

$$r / C_f = nK_b - K_b r \quad (1)$$

In eq. (1),  $r$  and  $n$  are binding density (equivalent to  $(C_t - C_f)/[\text{FTO}]$ ) and saturated adsorption amount of specific binding, respectively. As shown in Fig. 3b, the Scatchard plot bends at  $r = 0.006$  probably due to contribution of non-specific binding on the surface at high  $r$  region. The  $K_b$  for HRP calculated from linear regression at low  $r$  region (solid line) is  $5.4 \times 10^6 \text{ M}^{-1}$ , comparable to those of HRP (or different proteins) for other inorganic layered matrices.<sup>10,11,22</sup> Thus, the FTO nanolayer possesses a high affinity with the HRP molecules. As a matter of course, the FTO seems to be applicable as a host matrix not only for HRP but also other biomolecules.

Since the vibration bands of amide group of proteins are

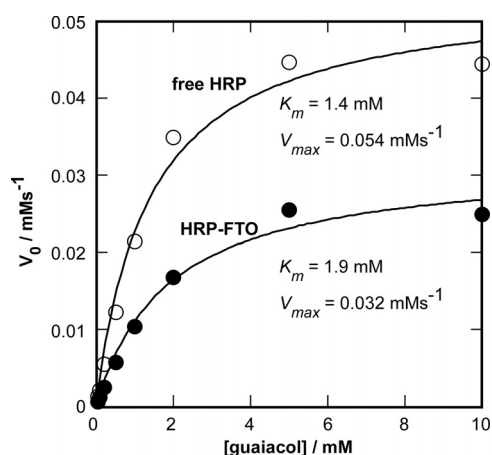


**Fig. 4** Peroxidase activities of free HRP and HRP bound to FTO. Initial reaction velocities ( $V_0$ ) of guaiacol and  $\text{H}_2\text{O}_2$  (1 mM) catalyzed by 1.5  $\mu\text{M}$  HRP in acetate buffer solution (pH = 4) are plotted as a function of guaiacol concentration. Solid lines indicate non-linear regression curves to determine kinetic parameters ( $K_m$  and  $V_{max}$ ).

sensitive to microstructural environment,<sup>15</sup> the FTIR spectra of HRP-FTO, native HRP, and original HFTO were collected to follow a conformational change of HRP during the hybridization (Fig. 2 in Supplementary Data). There is no change both in the amide I ( $1656 \text{ cm}^{-1}$ ) and the amide II ( $1541 \text{ cm}^{-1}$ ) bands after the reaction, suggesting that the hybridization process took place without any deformation of the secondary structure. The enzyme catalytic activities of free HRP and HRP-FTO nanohybrid were assayed for oxidation of *o*-methoxyphenol as a model substrate (Fig. 4). The absorption band (470 nm) of tetrameric products of the *o*-methoxyphenol under a presence of 1 mM  $\text{H}_2\text{O}_2$  was monitored as a function of time. The kinetic parameters ( $K_m$  and  $V_{max}$ ) for free and bound HRP (1.5  $\mu\text{M}$ ) were determined by curve fitting of the relationship between initial formation rate of the product and total substrate concentration. The  $V_{max}$  value of HRP-FTO is  $0.032 \text{ mM s}^{-1}$  while that of free HRP is  $0.054 \text{ mM s}^{-1}$ , suggesting that about 59 % of the activity remained even after the hybridization. The decrease of  $V_{max}$  may be indicative of steric restriction of the HRP molecules

interstratified between the rigid FTO layers.<sup>15</sup> Although detailed investigations to achieve higher peroxidase activity and stability than the free HRP are now progressing for various weight ratios of HRP and FTO, the obtained kinetic data here provide evidences that the bound HRP preserves a certain extent of peroxidase activity without serious denaturation and that the reactants and products of the catalytic reaction can access to the encapsulated HRP through the partly open framework.

In the past decade, it has been found out that several oxides doped with 3d magnetic elements including iron- and/or cobalt-doped layered titanates show ferromagnetism even at room temperature.<sup>23-25</sup> Therefore, biomolecule-magnetic layer nanohybrids synthesized in the present study are expected to become new magnetically applicable nanomaterials for biological uses.<sup>26</sup> The magnetization curves of HFTO and HRP-FTO were taken on a vibrating sample magnetometer (VSM) at room temperature (Fig. 5a). The clear

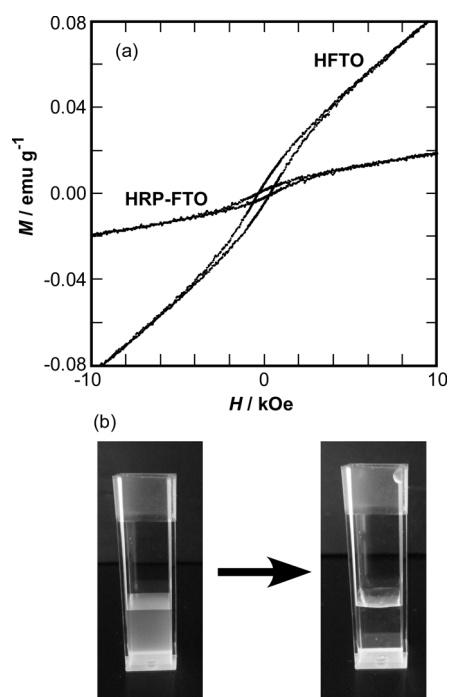


**Fig. 5** Magnetic properties of HRP-FTO nanohybrids. (a)  $M$ - $H$  curves of HFTO after annealing at 1073 K for 5 h in  $\text{N}_2$  and its nanohybrid with HRP (HRP / FTO = 2.5 (w/w)). (b) Photographs of HRP-FTO suspension (0.1 mg/ml) in cuvette before and after magnetic separation using neodymium magnets.

hysteresis loop appeared in the curves indicates that the HFTO and HRP-FTO possess an analogous magnetic property with the titanate layer doped with Co and/or Fe previously reported.<sup>24,25</sup> As compared with the HFTO, the reduced magnetization of the HRP-FTO reflects decreasing of FTO content in the powder. The tiny residual magnetization closed to the magnetite nanoparticles encapsulated in silica<sup>27</sup> appears to be advantageous to disperse the nanohybrids in solution without agglomeration. The photographs in Fig. 5b demonstrate a feasibility of magnetic separation of the HRP-FTO powder. A few ball-type neodymium magnets were

immersed into the HRP–FTO aqueous suspension (0.1 mg/ml) to collect the dispersed particles. It should be noted that most of HRP–FTO particles were trapped on the magnet surfaces and the suspension became colorless and transparent.  
5 Therefore, the prepared HRP–FTO nanohybrids are considered to be magnetically collectable. To our knowledge, this is the first example of magnetic separation for inorganic layer–biomolecule nanohybrid. Needless to say, titanate nanolayers excluding iron cannot be adsorbed on magnets.  
10 Recently, the other group reported that the layered double hydroxide (LDH) composed of magnetic elements as a scavenger of harmful anions can be recovered under applying an extremely high field generated by superconducting magnets.<sup>28</sup> On the other hand, the present HRP–FTO  
15 nanohybrids respond to relatively weak field with commercial magnets. This fact suggests that FTO has a great potential to be utilized for more efficient separation and facile manipulation processes.

## Conclusions

20 We have prepared nanohybrids of magnetic layered iron-titanate and enzyme HRP molecules via exfoliation-restacking process. It was found that HRP was electrostatically and spontaneously incorporated into the interlayer space of the nanolayers by adjusting the solution pH. The binding studies  
25 demonstrated the high affinity of iron–titanate for the HRP, and the enzyme preserved its activity after hybridization. The magnetic separation experiment indicated the formation of magnetically applicable inorganic layer–biomolecule nanohybrids. Thus, the magnetic layer–biomolecule  
30 nanohybrid will be a unique material which shows different properties from those of conventional biomolecule-immobilized magnetic particles.

## Acknowledgements

The present study was partly supported by Special  
35 Coordination Funds for Promoting Science and Technology, MEXT, Japan: “The Nagasaki University Strategy for Fostering Young Scientists”. The authors thank to Dr. T. Ohgai of Nagasaki University for assistance of the VSM measurements.

## Notes and references

<sup>a</sup> Department of Materials Science and Engineering, Faculty of Engineering, Nagasaki University, Nagasaki 852-8521, Japan; E-mail: kkmada@nagasaki-u.ac.jp

<sup>b</sup> Department of Applied Chemistry, Graduate School of Engineering, 45 Kyushu University, Fukuoka 819-0395, Japan; E-mail: soh@cstf.kyushu-u.ac.jp

† Electronic Supplementary Information (ESI) available: Figures showing SEM images FT-IR spectra of HRP-FTO nanohybrids. See DOI: 10.1039/b000000x/

50 1 R. Weissleder, A. Moore, U. Mahmood, R. Bhorade, H. Benveniste, E. A. Chiocca and J. P. Basilion, *Nat. Med.*, 2000, **6**, 351-355; J. W. M. Bulte, T. Douglas, B. Witwer, S.-C. Zhang, E. Strable, B. K. Lewis, H. Zywicke, B. Miller, P. van Gelderen, B. M. Moskowitz, I. D. Duncan and J. A. Frank, *Nat. Biotechnol.*, 2001, **19**, 1141-1147;  
55 2 M. Zhao, D. A. Beauregard, L. Loizou, B. Davletov and K. M. Brindle, *Nat. Med.*, 2001, **7**, 1241-1244; J. M. Perez, L. Josephson, T.

- O'Loughlin, D. Högemann and R. Weissleder, *Nat. Biotechnol.*, 2002, **20**, 816-820; Y.-M. Huh, Y.-w. Jun, H.-T. Song, S. Kim, J.-s. Choi, J.-H. Lee, S. Yoon, K.-S. Kim, J.-S. Shin, J.-S. Suh and J. Cheon, *J. Am. Chem. Soc.*, 2005, **127**, 12387-12391; Y.-w. Jun, J.-H. Lee and J. Cheon, *Angew. Chem. Int. Ed.*, 2008, **47**, 5122-5135.  
2 S. Giri, B. G. Trewyn, M. P. Stellmaker and V. S.-Y. Lin, *Angew. Chem. Int. Ed.*, 2005, **44**, 5038-5044; B. Wang, C. Xu, J. Xie, Z. Yang and S. Sun, *J. Am. Chem. Soc.*, 2005, **130**, 14436-14437; J.-H. Park, G. von Maltzahn, L. Zhang, A. M. Derfus, D. Simberg, T. J. Harris, E. Ruoslahti, S. N. Bhatia and M. J. Sailor, *Small*, 2009, **5**, 694-700.  
3 P. S. Doyle, J. Bibette, A. Bancaud and J.-L. Viovy, *Science*, 2002, **295**, 2237; D. Wang, J. He, N. Rosenzweig and Z. Rosenzweig, *Nano Lett.*, 2004, **4**, 409-413; T. Sen, A. Sebastianelli and I. J. Bruce, *J. Am. Chem. Soc.*, 2006, **128**, 7130-7131.  
4 L. R. Hirsh, R. J. Stafford, J. A. Bankson, S. R. Sershen, B. Rivera, R. E. Price, J. D. Hazle, N. J. Halas and J. L. West, *Proc. Natl. Acad. Sci. USA*, 2003, **100**, 13549.  
5 Y. Zhao, B. G. Trewyn, I. I. Slowing and V. S.-Y. Lin, *J. Am. Chem. Soc.*, 2009, **131**, 8398-8400; S. Hudson, J. Cooney and E. Magner, *Angew. Chem. Int. Ed.*, 2008, **47**, 8582-8594; A. Vinu, N. Gokulakrishnan, V. V. Balasubramanian, S. Alam, M. P. Kapoor, K. Ariga and T. Mori, *Chemistry-A Eur. J.*, 2008, **14**, 11529-11538; H.-A. Lin, C.-H. Liu, W.-C. Huang, S.-C. Liou, M.-W. Chu, C.-H. Chen, J.-F. Lee and C.-M. Yang, *Chem. Mater.*, 2008, **20**, 6617-6622; Y. Zhu, S. Kaskel, J. Shi, T. Wage and K.-H. van Pee, *Chem. Mater.*, 2007, **19**, 6408-6413.  
6 H. Takahashi, B. Li, T. Sasaki, C. Miyazaki, T. Kajino and S. Inagaki, *Chem. Mater.*, 2000, **12**, 3301-3305.  
7 K. Charradi, C. Forano, V. Prevot, A. Ben Haj Amara and C. Mousty, *Langmuir*, 2009, **20**, 10376-10383; A. J. Patil, E. Muthusamy and S. Mann, *J. Mater. Chem.*, 2005, **15**, 3838-3843; K. A. Carrado, S. M. Macha and D. M. Tiede, *Chem. Mater.*, 2004, **16**, 2559-2566; Y. Zhou, N. Hu, Y. Zeng and J. F. Rusling, *Langmuir*, 2002, **18**, 211-219; Y. Zhou, Z. Li, N. Hu, Y. Zeng and J. F. Rusling, *Langmuir*, 2002, **18**, 8573-8579.  
8 J.-M. Oh, S.-J. Choi, G.-E. Lee, S.-H. Han and J.-H. Choy, *Adv. Funct. Mater.*, 2009, **19**, 1617-1624; J.-H. Choy, S.-Y. Kwak, J.-S. Park, Y.-J. Jeong and J. Portier, *J. Am. Chem. Soc.*, 1999, **121**, 1399-1400; Q. Gao, S. L. Suib and J. F. Rusling, *Chem. Comm.*, 2002, 2254-2255.  
9 Y. Matsumoto, U. Unal, Y. Kimura, S. Ohashi and K. Izawa, *J. Phys. Chem. B*, 2005, **109**, 12748-12754; S. Ida, K. Araki, U. Unal, K. Izawa, O. Altuntasoglu, C. Ogata and Y. Matsumoto, *Chem. Comm.*, 2006, 3619-3621.  
10 C. V. Kumar and G. L. McLendon, *Chem. Mater.*, 1997, **9**, 863-870.  
11 C. V. Kumar and A. Chaudhari, *J. Am. Chem. Soc.*, 2000, **122**, 830-837.  
12 C. V. Kumar and A. Chaudhari, *Chem. Comm.*, 2002, 2382-2383; V. K. Mudhivarthi, A. Bhambhani and C. V. Kumar, *Dalton Trans.*, 2007, 5483-5497; A. Bhambhani and C. V. Kumar, *Micropor. Mesopor. Mater.*, 2008, **109**, 223-232.  
13 M. Harada, T. Sasaki, Y. Ebina and M. Watanabe, *J. Photochem. Photobiol. A*, 2002, **148**, 273-276.  
14 Q. Wang, Q. Gao and J. Shi, *J. Am. Chem. Soc.*, 2004, **126**, 14346-14347.  
15 Q. Wang, Q. Gao and J. Shi, *Langmuir*, 2004, **20**, 10231-10237.  
16 K. G. Welinder, *Eur. J. Biochem.*, 1979, **96**, 483-502.  
17 X. Chen, C. Fu, Y. Wang, W. Yang and D. G. Evans, *Biosens. Bioelectron.*, 2008, **24**, 356-361.  
18 T. Sasaki, M. Watanabe, Y. Michiue, Y. Komatsu, F. Izumi and S. Takenouchi, *Chem. Mater.*, 1995, **7**, 1001-1007; T. Sasaki, M. Watanabe, H. Hashizume, H. Yamada and H. Nakazawa, *J. Am. Chem. Soc.*, 1996, **118**, 8329-8335.  
19 L. Zhang, Q. Zhang, X. Lu and J. Li, *Biosens. Bioelectron.*, 2007, **23**, 102-106.  
20 C. V. Kumar, in *Handbook of Layered Materials*, ed. S. M. Auerbach, K. A. Carrado and P. K. Dutta, CRC Press, USA, 2004, ch. 7.  
21 K. A. Connors, in *Binding Constants – The Measurement of Molecular Complex Stability*, A Wiley-Interscience Publication, USA, 1987, ch. 2.

- 
- 22 S. Peng, Q. Gao, Q. Wang and J. Shi, *Chem. Mater.*, 2004, **16**, 2675-2684.
- 23 Y. Matsumoto, M. Murakami, T. Shiono, T. Hasegawa, T. Fukumura, M. Kawasaki, P. Ahmet, T. Chikyow, S.-y. Koshihara and H. Koinuma, *Science*, 2001, **291**, 854-856.
- 5 24 M. Osada, Y. Ebina, K. Takada and T. Sasaki, *Adv. Mater.*, 2006, **18**, 295-299; M. Osada, Y. Ebina, K. Fukuda, K. Ono, K. Takada, K. Yamaura, E. Takayama-Muromachi and T. Sasaki, *Phys. Rev. B*, 2006, **73**, 153301/1-153301/4.
- 10 25 Y. Kotani, T. Taniuchi, M. Osada, T. Sasaki, M. Kotsugi, F. Z. Guo, Y. Watanabe, M. Kubota and K. Ono, *Appl. Phys. Lett.*, 2008, **93**, 093112/1-093112/3.
- 26 G. Carja, H. Chiriac and N. Lupu, *J. Magn. Magn. Mater.*, 2007, **311**, 26-30.
- 15 27 C. Oh, Y.-G. Lee, C.-U. Jon and S.-G. Oh, *Colloids Surf. A*, 2009, **337**, 208-212.
- 28 A. Nakahira, T. Kubo and H. Murase, *IEEE Trans. Magn.*, 2007, **43**, 2442-2444.